Purification of Functionalized DNA Origami Nanostructures

Alan Shaw, Erik Benson, and Björn Högberg*

Department of Neuroscience and Department of Medical Biochemistry and Biophysics, Karolinska Institutet, Stockholm, Sweden

ABSTRACT The high programmability of DNA origami has provided tools for precise manipulation of matter at the nanoscale. This manipulation of matter opens up the possibility to arrange functional elements for a diverse range of applications that utilize the nanometer precision provided by these structures. However, the realization of functionalized DNA origami still suffers from imperfect production methods, in particular in the purification step, where excess material is separated from the desired functionalized DNA origami. In this article we demonstrate and optimize two purification methods that have not previously been applied to DNA origami. In addition, we provide a systematic study comparing the purification efficacy of these and five other commonly used purification methods. Three types of functionalized DNA origami were used as model systems in this study. DNA origami was patterned with either small molecules, antibodies, or larger proteins. With the results of our work we aim to provide a guideline in quality fabrication of various types of functionalized DNA origami and to provide a route for scalable production of these promising tools.

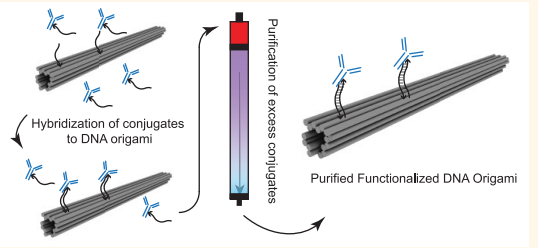

KEYWORDS: DNA origami · DNA nanostructures · purification · magnetic beads · FPLC · protein conjugation

The specificity of Watson–Crick base paring enables the arrangement of matter and function at the nanoscale with high programmability.[1,2] In particular, DNA origami[2,3] is one technique that has shown significant promise for applications because of its ease of design and production. Due to the programmability of the oligonucleotides that direct the folding of the structures (*i.e.*, the staples), it is possible to incorporate functional elements in the structures with high precision over stoichiometry and position. Examples of functionalized DNA origami can be seen in the field of drug delivery,[4–6] physics,[7,8] biophysics,[9–11] chemistry,[12,13] and cell biology.[14–16] Along with the increasing applications of functionalized DNA origami comes the need for robust methods for the production of desired functionalized DNA origami structures. Because functional groups are normally added in high excess to the structures, one of the crucial points is the purification step in which excess production materials are removed from the functionalized DNA origami to avoid interference in downstream experiments. For example, excess fluorophores could contribute to background noise in microscopy, and excess proteins can introduce background activity in cell biology studies unless properly removed from the structures. Note that here we are not investigating the removal of excess staple oligonucleotides, as this step is fairly well established.[7,15,17]

An additional difficulty arises when using molecules that display a wide range of nonspecific interactions with many surfaces, such as fluorophores and certain proteins.[18] These properties tend to render the functionalized structures sticky, and purification of these types of structures with increased nonspecific interactions (especially adhesion to membranes, resins, and plastics) becomes much more challenging, as an improper choice of purification method and material could result in poor recovery yield.

The model DNA origami structure used in this study is an 18-helix-bundle nanotube (further referred as 18HB), 13 nm in width and 138 nm in length with two pairs of protruding 21 nucleotide ssDNA at approximately 40 nm distance for conjugate hybridization[14] (Supporting Information Figure S1). Functionalization of the 18HB was done by first producing three types of conjugates, fluorophore, human IgG1 (immunoglobulin G 1), and ferritin, conjugated to an oligonucleotide

* Address correspondence to bjorn.hogberg@ki.se.

Received for review December 10, 2014 and accepted May 1, 2015.

Published online 10.1021/nn507035g

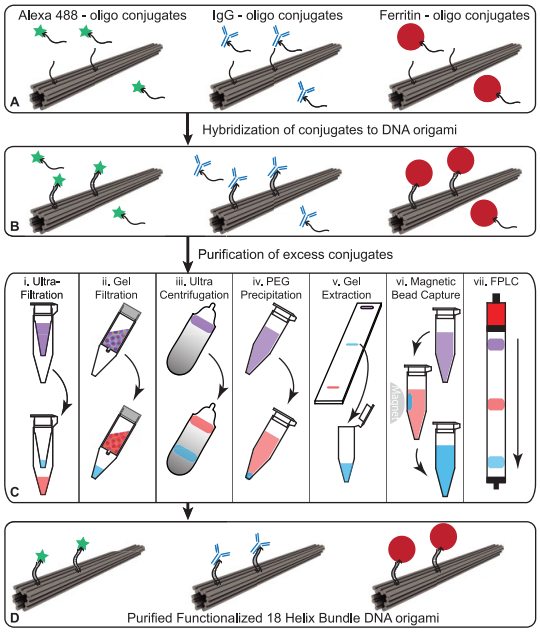

Figure 1. Workflow of the full production and purification of functionalized DNA origami used in this study. (A and B) Conjugates were mixed and hybridized to the 18HB; excess conjugates were still present in the sample. (C) The samples were purified with the seven different methods compared in this study. Purple indicates the mixture of excess conjugates with DNA origami, red indicates the fraction containing the excess conjugates, and blue indicates the fraction containing purified DNA origami. (D) Excess conjugates were removed, and purified functionalized 18HB was obtained.

that is complementary to the protruding sites on the 18HB and then further hybridizing the conjugates to the sites on the 18HB (Figure 1A,B).

The three model functional elements were chosen according to several potential applications and their peculiar characteristics: (1) Functionalized DNA origami structures with fluorescent response were used for microscopy studies.[17,19−22] The Alexa 488 fluorophore was chosen to represent purification of small molecules. (2) Addition of antibody fragments or Fc-chimeras to DNA origami structures can induce logic gated cell death[15] or be used to manipulate cell signaling.[14] An antibody (human IgG1) was chosen to represent medium-size proteins. (3) Ferritin can be clustered to alter MRI response[23] and was chosen to represent large proteins. Due to its larger size, excess ferritin during DNA origami production seems to be particularly difficult to remove.

A number of methods exist for the purification of DNA or protein.[24] In most cases these methods involve denaturing or breaking up the structure of either the DNA or the proteins. One of the difficulties in purifying DNA origami, in particular origami functionalized with protein, is that most existing methods destroy the nanoscale structure (*i.e.*, maintaining the pH, temperature, and salt conditions is crucial). Also, most available methods for size-based purification have been optimized for molecules on the order of kDa and not supramolecular assemblies on the order of MDa. Because of this, methods have been specifically tailored to purify DNA origami; these include PEG (poly(ethylene glycol)) precipitation,[25,26] gel extraction,[27] glycerol gradient ultracentrifugation,[17] size exclusion columns,[28] and spin filters.[15] However, there is a lack of a systematic study where different methods are compared to each other using similar types of samples.

Here we systematically examine and optimize these five common purification methods, together with two methods previously unreported for DNA origami; for an overview see Figure 1C. The compared methods are (i) ultrafiltration, where a repetitive dilution-concentration process across a regenerated cellulose membrane of a certain molecular weight cutoff, which retains the large DNA origami structures while the small contaminants flow through;[15] (ii) gel filtration with spin columns, where various dextran- or agarose-based size exclusion resins in spin columns will retain contaminants while DNA origami structures flow through in the void volume during centrifugation;[28] (iii) glycerol density gradient ultracentrifugation, where DNA origami structures and contaminants are separated by density as they are forced through a glycerol density gradient by high-speed centrifugation;[17] (iv) PEG precipitation, where different PEG w/v % are used to pellet the DNA origami structures or contaminants;[9,23] (v) agarose gel extraction, where DNA origami structures are first electrophoresed and the corresponding gel bands containing the structures are cut out and gel extracted. The two methods we adapted for DNA origami are (vi) magnetic bead capture−release of DNA origami, for a potentially universal purification method for functionalized DNA origami, and (vii) fast protein liquid chromatography (FPLC) using a Superose 6 column.

The magnetic bead capture method utilizes DNA strand invasion to purify functionalized DNA origami. In this reaction, one DNA strand is substituted by a longer competitive strand, and it can thus be used to displace hybridized bonds without resorting to denaturing conditions.[29] We modified the 18HB to have linker oligonucleotides protruding from one end of the structure. The linker sequence protruding out of the structure consists of two parts: a poly-A tail, which binds to the poly-T sequence on the magnetic bead, and an invader oligonucleotide toehold sequence. Structures were first bound to the magnetic beads *via* hybridization, and unbound excess conjugates were then washed away. The structures were subsequently released by the addition of invader oligonucleotides; these oligonucleotides first bind to the toehold region on the linker and eventually replace the region of the 18HB originally hybridized to the linker, thus releasing the DNA origami (Figures 1C, 2A; sequences used in this method are given in the Materials and Methods section).

For the FPLC method, we applied an FPLC system equipped with size exclusion columns to purify the

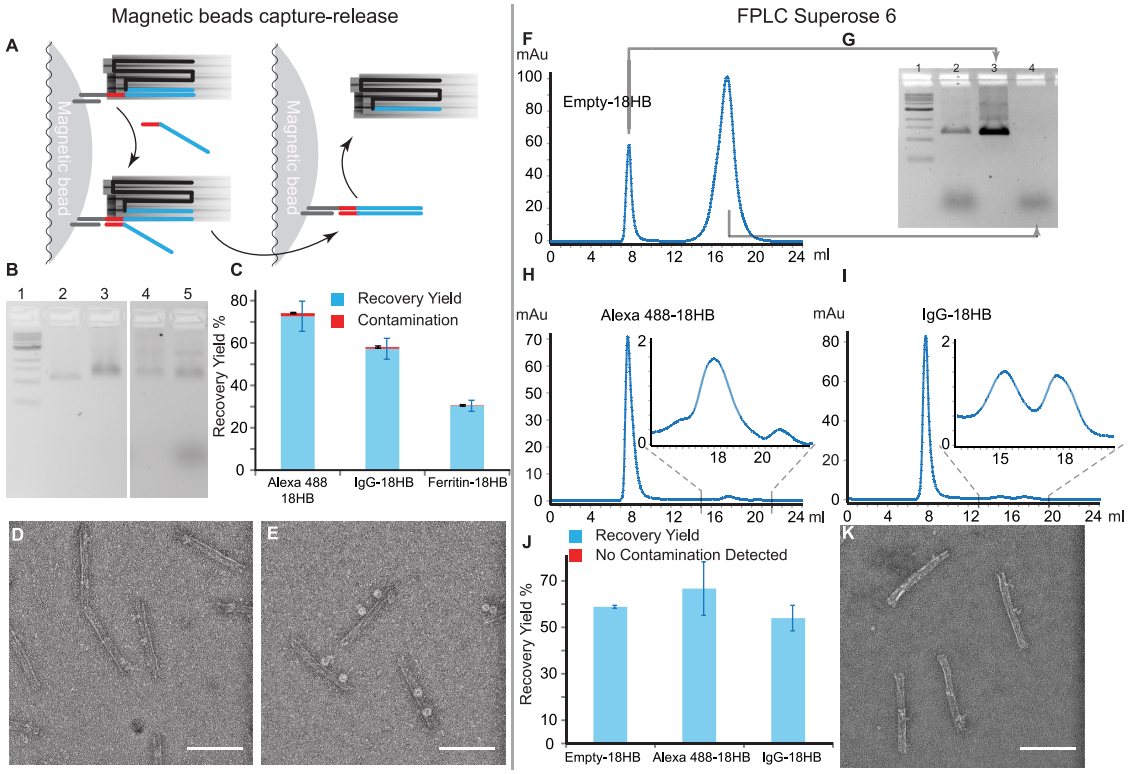

Figure 2. Summary of the two methods adapted for DNA origami in this study. (A) Magnetic beads modified with poly-T oligonucleotides (gray lines) were hybridized to linker oligonucleotides (the gray-red-blue line) on the 18HB. After capture and removal of excess conjugates an invader (red-blue line) was added, binding to the red toehold region on the linker and displacing the blue sequence, releasing the 18HB. (B) A 2% agarose gel demonstrating the purification with the magnetic bead method: (1) 1kb ladder, (2) empty 18HB, (3) unpurified IgG-18HB, (4) initial fraction from magnetic bead capture, (5) eluted IgG-18HB from magnetic bead capture. (C) Summary of recovery yield (blue columns) and contamination (red columns). Error bars (black: contamination, blue: recovery yield) represent standard deviation of the mean (SDM). TEM micrographs of magnetic bead capture purified IgG-18HB (D) and ferritin-18HB (E); scale bars are 100 nm. Chromatogram showing the separation of (F) excess staples with empty 18HB. (G) A 2% agarose gel supporting the separation between empty 18HB and excess staples in F: (1) 1kb ladder, (2) unpurified 18HB, (3) samples from the peak at 8 mL, (4) samples from the peak at 17 mL. Chromatograms demonstrating the separation of (H) excess Alexa 488 conjugates and (I) excess IgG conjugates from the functionalized 18HB; insets in H and I are expansions of the peaks of the excess conjugates. (J) Summary of purification results with FPLC; error bars represent SDM. (K) TEM micrograph of FPLC-purified IgG-18HB; the scale bar is 100 nm.

functionalized 18HB. This technique is commonly used to purify plasmid DNA or proteins. While other chromatography methods, such as ion exchange and affinity purification, often require high ionic strength buffer to elute the molecules of interest, size exclusion chromatography can be performed in a variety of biologically compatible buffers, such as phosphate-buffered saline (PBS) and tris-buffered saline (TBS). We performed size exclusion chromatography with the Superose 6 column; this column has a fractionation range between 5×10^3 and 5×10^6 Da, which in principle should make it an optimal candidate for separating smaller conjugates (mol wt between 7×10^3 and 2×10^5 Da) from the functionalized 18HB (mol wt $\approx 5 \times 10^6$ Da). Size exclusion chromatography with the Superose 6 column can process up to 500 μL in a single cycle.

RESULTS AND DISCUSSION

To determine the purification efficiency of all methods, we performed the experiments at each method's optimal sample volume, which is either 50 μL or 100 μL of 20 nM 18HB. For each functionalized 18HB, agarose gel electrophoresis (AGE) was used to examine the integrity of the DNA origami structure. TEM micrographs of purified samples are given in Figure 2 and Supporting Information Figure S2, to complement the AGE. The recovery yield was calculated by the gel band intensity of purified functionalized 18HB using unpurified functionalized 18HB as reference (Supporting Information Figure S3) and expressed in percentage. The change in sample volume before and after purification was recorded. The contamination was quantified by applying the same purification protocols on samples containing only conjugates. Alexa-488 conjugates were quantified by comparing fluorescence intensity. IgG conjugates were quantified by silver staining on denaturing PAGE. Ferritin conjugates were quantified by the Bradford assay. The contamination is expressed as the percentage of contaminants remaining in the sample after purification compared to the unpurified sample.

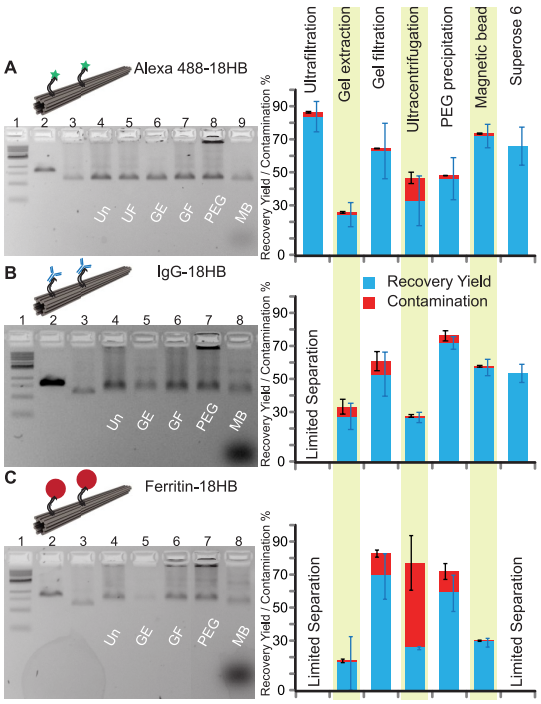

Figure 3. Summary of the recovery yield and contamination of all purification methods used in this study. (A) Purification of Alexa 488-18HB. (B) Purification of IgG-18HB. (C) Purification of ferritin-18HB. Left panel: AGE of one of the repeats for each functionalization type: (1) 1kb ladder, (2) p7560 ssDNA, (3) empty-18HB, (4) unpurified functionalized 18HB. For 5−9 in (A) Alexa 488-18HB purified with (5) ultrafiltration, (6) gel extraction, (7) gel filtration, (8) PEG precipitation, and (9) magnetic bead capture. For 5−8 in (B) and (C), IgG-18HB and ferritin-18HB purified with (5) gel extraction, (6) gel filtration, (7) PEG fractionation, (8) magnetic bead capture. Right panel: Average recovery yield of three repeats is presented as blue columns, and the contamination is presented as red columns. Three repeats were done for each method for each functionalization type. Error bars (black for contamination, blue for recovery yield) represent SDM. AGE of functionalized 18HB purified with ultracentrifugation is shown in Supporting Information Figure S13. Un, unpurified functionalized 18HB; UF, ultrafiltration; GE, gel extraction; GF, gel filtration; PEG, PEG precipitation; MB, magnetic bead.

Results from the magnetic bead capture method and the FPLC method are shown in Figure 2; a comparison between the two new techniques we adapted and the five common purification methods is shown in Figure 3. For each functionalization type, three repeats were done for each purification method.

The recovery yield for the samples purified with the magnetic bead capture method is around 70% for Alexa 488-18HB, 57% for IgG-18HB, and 30% for ferritin-18HB (Figure 2B). While the recovery yield for Alexa 488-18HB and IgG-18HB is comparable to that of the common methods shown in Figure 3, it is lower for ferritin-18HB, which we suspect is due to nonspecific interaction between the magnetic beads and ferritin. IgG also interacts nonspecifically with the beads, but in this case we were able to reduce the nonspecific interaction by adding poloxamer, a nonionic block copolymer of ethylene glycol and oxypropylene, which is often used in cell culture systems with constant stirring or liquid flow[30] (Supporting Information Figure S4). However, for ferritin, the nonspecific interaction with the beads could not be reduced *via* the addition of poloxamer. The conjugate contamination in samples purified with the magnetic bead method is lower than the majority of the common purification methods; a column plot for comparison is shown in Figure 3.

If the excess invader oligonucleotides need to be removed, we present an alternative step, where the invader oligonucleotide is biotinylated and becomes easily removable by incubating the eluted sample with streptavidin magnetic beads. The DNA origami structure remains intact during this additional step (Supporting Information Figure S5).

In summary, the magnetic bead capture method exhibits superior purity and comparable recovery yield compared to the common methods we investigated. The purity of the samples is independent of the functional elements, as all Alexa 488, IgG, and ferritin conjugates resulted in similar purity. Derived from these results, we suggest that this method is potentially a universal purification method for functionalized DNA origami, which can offer high-purity samples in a wide spectrum of functionalization applications.

In initial FPLC experiments we observed suboptimal recovery yield of the DNA origami structures, which we suspect is the result of two effects: first, Mg^{2+} bridging the negative DNA backbone with the hydroxyl lone pairs on the agarose-based Superose resin. Second, on the surface of the DNA origami structures are densely packed phosphates, which make the local charge concentration relatively higher when compared to the free M13 plasmid alone. We hypothesize that the combination of these two effects limits the recovery yield of DNA origami structures and can be supported by comparing the recovery yield of the 18HB with that of the M13 plasmid (entries 9 and 10 in Supporting Information Table S1). Under the same buffer conditions, the recovery yield for the M13 plasmid is 171% higher than the 18HB. To overcome this effect, we tested buffers with various compositions and concentrations of ions (Supporting Information Table S1). We discovered that within all salt conditions tested, the recovery yield is most sensitive to [Mg^{2+}]; when its concentration was decreased from 10 mM to 3 mM, the recovery yield increased from 11% to 58%. Sodium ion concentration also played a role in the recovery yield; when its concentration was increased from 150 mM to 200 mM, the recovery yield increased from 55% to 61% when TBS was used as running buffer. A 1× PBS solution with 3 mM $MgCl_2$ was chosen as the running buffer for further experiments.

We separately injected empty 18HB or conjugates alone to examine their respective retention volumes. As shown in Figure 2F−I, empty 18HB elutes at 8 mL,

excess staples from DNA origami folding elute at 17 mL (Figure 2 F,G), Alexa488 conjugates elute at 18 mL, and IgG conjugates elute at 15 and 18 mL, indicating good resolution for separating DNA origami nanostructures with the two conjugates. The chromatograms (Figure 2H,I) show that the functionalized 18HBs are well separated from the excess conjugates, and the recovery yield is in the range of 50% to 60%, which is comparable to some of the common methods (Figure 3).

Ferritin, however, due to its larger hydrodynamic radius, elutes at several peaks, with the first peak overlapping with the 18HB (Supporting Information Figure S6 left panel), and thus the Superose 6 column cannot be used to purify ferritin from origami. In an attempt to overcome this issue, we tried a Sephacryl S500 column instead. Initial data from these experiments (see Supporting Information Figure S6 right panel) indicate that a full separation of ferritin-functionalized 18HB from the excess ferritin conjugates is possible using the S500 column.

One potential problem in DNA origami production can be the creation of multimers during folding. We were interested to see whether the FPLC could be used to enrich the monomeric samples. In our hands, we were unable to separate the monomers and dimers using the Sephacryl S500 column. In fact, we observed that the two samples elute in the same peak at 50 mL (Supporting Information Figure S7).

The five common, previously published, purification methods were first further fine-tuned to achieve optimal purification efficacy for equal comparison. Some methods are carried out with different reagent or resins, so we first preformed one repeat of each (Supporting Information Figure S8), and the most successful reagent or resin was chosen and further compared to the other methods.

Ultrafiltration filters can be passivated with proteins or chemicals to reduce nonspecific interactions with the sample. BSA (bovine serum albumin), Tween, and milk powder have been described to serve this purpose. However, the previously described passivation methods suffer from some shortcomings: passivation with BSA potentially blocks the membrane pores, reducing its purification efficiency; Tween and other surfactants are cytotoxic and notorious for forming micelles, which are challenging to remove and the presence of which might introduce toxicity problems if the aim is to apply these samples to cell culture or living organisms. However, we discovered that poloxamer performs well as a passivation reagent. Ultrafiltration filters passivated with poloxamer (described above) exhibit higher recovery yield and at the same time maintain the filter's purification efficiency (Supporting Information Figure S8).

Agarose gel extraction is arguably the most widely used method for purifying DNA origami, but it requires extensive hands-on time and has a low recovery yield. While separation of Alexa 488 and IgG conjugates from the 18HB was achieved, ferritin conjugates run at the same speed as the 18HB in the gel. In order to circumvent this problem, we replaced the basic TBE gel running buffer with an acidic TAE running buffer, and we performed AGE at pH 4, which is close to the theoretical pI of ferritin, and recovered the ferritin-18HB by gel extraction. By doing this, we were able to achieve separation between ferritin and the ferritin-functionalized 18HB (Supporting Information Figure S9).

There is a wide variety of gel filtration resins with different physical and chemical properties. The DNA origami nanostructures folded from the M13 phage genome are normally large enough to be eluted in the void volume in gel filtration with spin columns, while smaller particles such as oligonucleotides and conjugates will be retained in the resin. We discovered that, like the issue with magnesium in FPLC columns, the presence of magnesium reduces the recovery yield of the DNA origami. In order to circumvent this issue, we used a different approach: the resins were equilibrated in PBS without magnesium, but the lack of magnesium in the eluted sample solution would eventually lead to denaturation of the DNA origami. To cope with this issue, we pipetted a 1 μL droplet of 1 M $MgCl_2$ at the bottom of the collection tube before the collection spin (Supporting Information Figure S10) so that the eluted structures would immediately be replenished with magnesium during the spin.

PEG precipitation often results in sample aggregation (lane 6, Supporting Information Figure S3), probably due to the extensive concentration during the process. Despite this method's drawback, we demonstrated that PEG precipitation could be a powerful method to remove aggregates from monomeric samples. By using a low concentration of PEG (0.5−1.0% w/v) we were able to selectively pellet the aggregates formed during an unoptimal folding of the 18HB, while the monomeric 18HB remains intact in the supernatant (Supporting Information Figure S11).

For purification of Alexa 488-18HB, the three methods that gave the best recovery yield are ultrafiltration filters passivated with poloxamer, magnetic bead capture, and gel filtration, which gave an average recovery yield of 84%, 72%, and 63%, respectively. These methods also provided very pure samples, being able to remove near 98% of excess Alexa488 conjugates.

For purification of IgG-18HB, the three methods that gave the best recovery yield are PEG precipitation, magnetic bead capture, and gel filtration, which gave an average recovery yield of 72%, 57%, and 53%, respectively. Magnetic bead capture and ultracentrifugation were able to remove near 98% of excess IgG conjugates.

For purification of ferritin-18HB, the two methods that gave the best recovery yield are gel filtration and PEG precipitation, which gave an average recovery yield of 70% and 60%, respectively. Due to ferritin's

larger size, all purification methods were less efficient in removing excess ferritin, except the magnetic bead capture, which removed >99% of the excess ferritin conjugates.

Methods that involve pelleting or concentration of samples have a higher tendency to aggregate the samples during the purification process. As shown in Figure 3, samples purified with ultrafiltration or PEG precipitation have an increased smear or aggregation. We used TEM to image purified ferritin-18HB to examine the integrity of the structures after purification. We found no major difference in the site occupancy between purification methods and the unpurified sample (Supporting Information Figure S12), which indicates that the integrity of the functionalized 18HB was retained during the purification processes.

CONCLUSIONS

In summary, we have developed two methods that have not previously been applied to DNA origami nanostructures, demonstrated their efficiency to purify functionalized DNA origami, and systematically compared them to five other common purification methods in the removal of three types of useful functionalization conjugates. Magnetic bead capture is a potential universal purification method for DNA origami, as its purification efficiency is independent of the contaminant's chemical or physical properties, and it possesses a comparable recovery yield when compared to the common methods. FPLC is a powerful and automated method for scale-up production of functionalized DNA origami. By careful choice of size exclusion columns, full separation of contaminants and functionalized DNA origami is achievable. Together with scalable enzymatic production of oligonucleotides,[31] this method provides a route for larger scale applications such as biomedical studies using functionalized DNA origami. Our results provide a general guideline for choosing the optimal purification method for various applications, as well as new insights in the production of functionalized DNA origami.

MATERIALS AND METHODS

Production of the 18-Helix Bundle. *p7560 Scaffold ssDNA Preparation.* A single colony of *E. coli* JM109 was cultured to saturation overnight in 25 mL of lysogeny broth (LB, VWR). From this, 3 mL was diluted to 253 mL in 2× YT medium (VWR) supplemented with 5 mM $MgCl_2$ (VWR) and cultured in a 37 °C shaker. Optical density at 600 nm was measured continually and until a value of 0.5 was reached. At this point p7560 phages were added at a multiple of infection (MOI) of 1, and incubation was continued for 5 h. The culture was transferred to a centrifuge bottle and was centrifuged at 4000*g* for 30 min at 4 °C. The supernatant was saved and centrifuged again at the same conditions. The supernatant was recovered, 10 g of PEG 8000 (VWR) and 7.5 g of NaCl (VWR) were added, and the mixture was then incubated on ice for 30 min and centrifuged at 10000*g* for 40 min at 4 °C. After centrifugation, the supernatant was discarded; the pellet was resuspended in 10 mL of 10 mM Tris (pH 8.5, VWR) and transferred to a 85 mL centrifuge bottle (VWR). A 10 mL amount of 0.2 M NaOH (Sigma-Aldrich) and 1% SDS (VWR) were added, mixed gently by inversion, and incubated at room temperature for 3 min. Then 7.5 mL of 3 M KOAc (VWR), pH 5.5, was added, and the mixture was mixed gently by swirling and incubated on ice for 10 min. The mixture was centrifuged at 16500*g* for 30 min. The supernatant was poured into fresh centrifuge bottles, 50 mL of 99.5% EtOH (Kemethyl) was added, and the mixture was gently mixed by inversion and incubated on ice for 30 min. The solution was centrifuged at 16500*g* for 30 min to precipitate the DNA. After decanting the supernatant, the DNA pellet was washed with 75% EtOH (Kemethyl) and air dried at room temperature for 15 min. Finally, the pellet was resuspended in 1.5 mL of 10 mM Tris (pH 8.5), and the concentration and quality of p7560 ssDNA were characterized by UV−vis (Nanodrop, ThermoScientific) and a 1.5% agarose gel with 10 mM $MgCl_2$, respectively.

Staple Oligonucleotide Preparation. Oligonucleotides were purchased from Bioneer (South Korea) in 96-well plates on a 6 nmol synthesis scale. The staples in each well were resuspended and diluted in water to a final concentration of 100 μM. The final concentration of the staples after pooling was adjusted to 400 nM each.

Folding of 18HB and Removal of Excess Staples. The standard folding conditions used in this study were as follows: 20 nM ssDNA scaffold, 100 nM each staple, 13 mM $MgCl_2$, 5 mM Tris pH 8.5, and 1 mM EDTA. Folding was carried out by rapid heat denaturation followed by slow cooling from 80 to 60 °C over 20 min, then 60 to 24 °C for 14 h. Removal of excess staples was done by washing (repetitive concentration/dilution) the 18HB with PBS pH 7.4 supplemented with 10 mM $MgCl_2$ in 100 kDa MWCO 0.5 mL Amicon centrifugal filters (Merck Millipore). In more detail the 18HB solution was diluted to 450 μL, transferred to a prewetted centrifugal filter, and centrifuged at 14000*g*, 15 °C for 2 min, then diluted again to 450 μL, mixed well, and centrifuged again under the same conditions. The volume was adjusted with PBS pH 7.4 (10× from Sigma-Aldrich) and 10 mM $MgCl_2$ to a 18HB concentration of 20 nM, and the sample was collected *via* centrifugation at 1000*g* for 2 min. To remove excess staples, the 18HB samples were washed five times.

Production of Alexa488, IgG1, and Ferritin Oligonucleotide Conjugates. An Alexa 488-modified oligonucleotide was purchased from Bioneer (South Korea). IgG1 and ferrtin oligonucleotide conjugates were produced as described below.

4FB Modification of 3′-Amino-Modified Oligonucleotide. The 3′-amino-modified oligonucleotides (Bioneer) were resuspended and diluted to 0.2 mM in reaction buffer (0.5 mM EDTA pH 8), washed with the same buffer three times in a Vivaspin 5 kDa MWCO spin filter (centrifuged at 15000*g*, 12 min, room temperature, Sartorius), and concentrated to 23 μL (2 mM of the oligonucleotide concentration). To this solution was added 12.5 μL of 0.172 M Sulfo-S-4FB (Solulink) in DMF, and the mixture was incubated for 1 h at room temperature with occasional mixing. This procedure was repeated once. The reaction mixture was diluted with conjugation buffer (1× PBS pH 6.0), transferred to a Vivaspin 5 kDa MWCO spin filter (prewetted with conjugation buffer), washed with the same buffer seven times (centrifugation at 15000*g*, 12 min, room temperature), and concentrated to 20 μL. The 4FB-modified oligonucleotide was then stored at 4 °C overnight.

HyNic Modification of Ligand and Conjugation of Modified Ligand with Modified Oligonucleotide. A 200 μg amount of lyophilized human IgG1 (recombinant human IgG1 Fc, R&D Systems) was dissolved in 100 μL of PBS, pH 7.4. The IgG1 solution was buffer exchanged to PBS pH 7.4 using a Zebaspin desalting column, 7 kDa MWCO (Thermo Fisher Scientific). A 2 μL portion of 7.3 μM Sulfo-S-HyNic (Solulink) in DMF (Sigma-Aldrich) was added, and the mixture was incubated at room temperature for 2 h with occasional mixing. The ligand solution was buffer exchanged to PBS pH 6.0 using a Zebaspin desalting

column, 7 kDa MWCO, 10 μL of the 4FB-modified oligonucleotide (*ca*. 10 time excess) was added, and the mixture was incubated for 2 h at room temperature with occasional mixing. Upon completion, the antibody conjugate solution was diluted with PBS pH 7.4 to 450 μL, transferred to an Amicon ultrafiltration unit, 50k MWCO, and washed four times with PBS pH 7.4. After the final wash the volume was adjusted to 100 μL. To evaluate the efficiency of conjugation of IgG1 to DNA, the absorption of light at 350 nm was measured, giving an estimate of the ligand-to-oligonucleotide ratio.

Functionalization of the 18-Helix Bundle. The three different types of conjugates were added with a 3-fold excess to each protruding oligonucleotide on the 18HB with a final 18HB concentration of 20 nM, and the crude mixture was incubated in the PCR machine with a temperature ramp starting from 1 h at 37 °C followed by 14 h at 22 °C. Immediately after incubation the functionalized 18-helix bundle was stored at 4 °C until further purification.

Purification with Amicon Centrifuge Filters. Passivation of the Amicon filters was carried out by incubating the filters in passivation buffer (1× PBS and 2% BSA (Sigma-Aldrich) in PBS or 5% Pluronics (Sigma-Aldrich) in water) at room temperature overnight, and then the filters were washed with diH_2O three times before the crude mixture was transferred into it. The 100 μL crude 18-helix bundle mixture was diluted to 500 μL with 1× PBS supplemented with 10 mM $MgCl_2$ and transferred to the passivated and washed filters. The filters were spun at 15 °C, 14000*g* for 2 min. The retention was diluted to 500 μL again by adding 1× PBS supplemented with 10 mM $MgCl_2$ and spun again under the same conditions. A total of six washes were performed. After the final wash the filters were reversed, placed in a fresh tube, and spun at 15 °C 1000*g* for 2 min. The purified 18-helix bundle was then collected for further characterization.

Purification with Agarose Gel Extraction. A 2% agarose (VWR) gel supplemented with 10 mM $MgCl_2$ was casted with extra-long wells, 0.5× TBE buffer (Tris base, boric acid, EDTA purchased from VWR) supplemented with 10 mM $MgCl_2$ was used as running buffer, the whole gel case was then placed in an ice−water bath, and the gel was electrophoresed at 70 V for 3.5 h. A 4 μL amount of the crude 18-helix bundle mixture was loaded in the small center well for reference, and 100 μL of functionalized 18-helix bundle mixture was loaded into the long well for extraction. All samples were mixed with a 25% volume of agarose gel loading dye (30% glycerol, 10 mM Tris, 1 mM EDTA, 0.25% bromophenyl blue). Upon completion the reference lane was cut out and post stained with ethidium bromide (1 μL of 1 mg/mL to 20 mL of buffer) and placed back into the gel as a reference for gel cutting. The cropped out gel was then chopped into small pieces, placed into a freezer for 20 min, and finally spun at room temperature, 13000g for 20 min. The collected filtrate was then concentrated with a 5% pluronic passivated Amicon filter, 100kda MWCO.

Purification with Size Exclusion Spin Columns (Gel Filtration). The size exclusion resins (Sigma-Aldrich) were buffer exchanged by repetitive resuspension/pelleting in 1× PBS six times (10 mL of crude resin was diluted to 50 mL with 1× PBS and spun at 800*g* for 3 min) and transferred to a 15 mL Falcon tube to adjust the resin to a 50% v/v slurry. The resins were then loaded into Thermo empty spin columns (Thermo Scientific) with the suitable volume for different contaminants, and excess buffer in the resin was removed by spinning the columns at 15 °C, 800*g* for 1 min. The crude 18HB mixture was then subsequently passed through two spin columns (spun at 800*g* for 3 min) with different resin volumes (400−260 μL for Alexa 488 samples; 400−280 μL for IgG 1 samples; 400−300 μL for ferritin samples) with 1 μL of 1 M $MgCl_2$ at the bottom of the collection tube. The purified samples were then concentrated with 5% pluronic passivated Amicon filters.

Purification with Glycerol Ultracentrifugation. A 1.6 mL volume of folding buffer suplemented with 45% glycerol (VWR) was transferred to a polyallomer centrifuge tube (Beckman #355870). A 1.6 mL volume of folding buffer supplemented with 15% glycerol was then carefully layered on top. The tube was capped and positioned horizontally for 60 min to establish a density gradient. A 100 μL amount of sample was brought to 10% glycerol concentration and carefully loaded on top of the gradient. The tube was loaded in a Beckman SW-41Ti rotor and centrifuged at 35 000 rpm for 1 h 45 min at 4 °C. After centrifugation, a long-neck gel loading pipet tip was used to split the gradient in nine or 10 fractions from the top. A sample from each fraction was loaded in an agarose gel to find what fractions contain the DNA structures. The fractions containing the structures were pooled and washed in folding buffer using Amicon filters as previously described.

Purification with PEG Fractionation. 18HB samples (50 μL) were mixed with 12.5 μL of 17.5% PEG 8000 (VWR), 500 mM NaCl, and 10 mM $MgCl_2$, incubated at 4 °C for 10 min, and centrifuged at 4 °C for 30 min at 12600*g*. Supernatant was removed, and the pellet was resuspended in 50 μL of buffer (PBS pH 7.4 with 10 mM $MgCl_2$). Another 12.5 μL of the PEG solution was added, and the whole step was repeated once more. Finally the pellet was resuspended in 50 μL of buffer.

Purification with Magentic Bead Capture. A 300 μL amount of crude solution of Dynabeads conjugated with poly-T oligonucleotides (Invitrogen) was transferred to an Eppendorf tube and placed on a magnet. The original storage buffer was removed, and the Dynabeads were resuspended in 75 μL of PBS + 10 mM $MgCl_2$; this solution is further referred to as 4× Dynabeads. Then 16.5 μL of 4× Dynabeads was added to 50 μL of 18HB, and the mixture was placed on a rotating mixer overnight at room temperature. Afterward the tube was placed on a magnet, the supernatant was removed, and the beads were washed two times with PBS + 10 mM $MgCl_2$ and resuspended in 50 μL of buffer. A 0.8 μL amount of 100 μM invader strands was added to the resuspended beads, and the tube was placed again on the rotating mixer for 7 h. Finally the tubes were placed on a magnet, and the supernatant that contains the eluted 18HB was collected.

The optional step to remove excess invader strands was carried out as follows: in the elution step, use invader oligonucleotide modified with 3′ biotin. After collecting the eluted solution from the Dynabeads, add 20 μL of 5× streptavidin Dynabeads (Invitrogen) to the eluted solution and incubate for 15 min. Finally remove the streptavidin Dynabeads with a magnet.

The sequences used in the magnetic bead capture method are as follows: linker 1: 5′ CTGAAAGCGTAAGAATACGCTGGCTTGCCAAAAAAAAAAAAAAAAAAAAAAAA 3′; linker 2: 5′ CCATTAAAAATACCGAACGAACCGTGCGTCTCCAAAAAAAAAAAAAAAAAAAAAAAA 3′; invader 1: 5′ GGCAAGCCAGCGTATTCTTACGCTTTCAG 3′; invader 2: 5′ GGAGACGCACGGTTCGTTCGGTATTTTTAATGG 3′.

FPLC Purification of the 18HB. The Akta pure FPLC (GE Healthcare) system was equipped with a Superose 6 column (GE Healthcare) or a Sephacryl S500 column (GE Healthcare). The flow rate was set to 0.4 mL/min for Superose 6 (GE Healthcare) and 0.15 mL/min for Sephacryl S500 (GE Healthcare). The column was coupled to a 280 nm UV spectrophotometer and a fraction collector, which collects 0.5 mL fractions for the Superose 6 column and 3 mL for the Sephacryl S500 column. Samples were injected manually with a syringe.

Calculation of Recovery Yield and Contamination. For the calculation of functionalized 18HB recovery yield, an unpurified "crude" sample and the purified samples were eletrophoresed in a 2% agarose gel, prestained with EtBr, and the gel band intensity of the 18HB band was measured with Image J. Since we know the amount of sample loaded in the reference lane, we can easily calculate the amount of 18HB in the purified sample lanes and thus calculate the concentration of the 18HB in the purified samples. By recording the change in sample volume before and after purification we then are able to calculate the recovery yield of the 18HB.

Calculation of conjugates' contamination was carried out in different ways depending on the conjugate. The fluorescence intensity of purified Alexa 488 samples was compared to unpurified references; IgG samples were run in a 10% denaturing PAGE and post stained with a silver staining kit (GE Healthcare). The Fc band intensity of the purified samples was compared to that of an unpurified reference. The concentration of purified ferritin samples was measured with the

Bradford assay (Bio-Rad) using an unpurified ferritin sample as reference.

Conflict of Interest: The authors declare no competing financial interest.

Supporting Information Available: Structure designs, DNA sequences, additional TEM images, agarose gel images, FPLC chromatograms. The Supporting Information is available free of charge on the ACS Publications website at DOI: 10.1021/nn507035g.

Acknowledgment. We would like to thank Ana Edvardsson for help with the Akta pure system, and GE Demo lab in SciLifeLab for lending us the Akta pure system. All authors would like to thank all members of the Högberg lab for fruitful discussions. The work was financed through the Swedish Research Council (grants 2010-5060 and 2013-5883 to B.H.), the Swedish Foundation for Strategic Research (grant FFL12-0219 to B.H.), and Knut and Alice Wallenberg's foundation (Academy Fellows grant KAW 2014.0241 to B.H.). A.S. is partly financed by a faculty grant from Karolinska Institutet (KID-funding).

REFERENCES AND NOTES

1. Jones, M. R.; Seeman, N. C.; Mirkin, C. A. Programmable Materials and the Nature of the DNA Bond. *Science* **2015**, *347*, 1260901–1260911.
2. Rothemund, P. W. K. Folding DNA to Create Nanoscale Shapes and Patterns. *Nature* **2006**, *440*, 297–302.
3. Douglas, S. M.; Dietz, H.; Liedl, T.; Högberg, B.; Graf, F.; Shih, W. M. Self-Assembly of DNA into Nanoscale Three-Dimensional Shapes. *Nature* **2009**, *459*, 414–418.
4. Jiang, Q.; Song, C.; Nangreave, J.; Liu, X.; Lin, L.; Qiu, D.; Wang, Z.-G.; Zou, G.; Liang, X.; Yan, H.; *et al*. DNA Origami as a Carrier for Circumvention of Drug Resistance. *J. Am. Chem. Soc.* **2012**, *134*, 13396–13403.
5. Zhao, Y.; Shaw, A.; Zeng, X.; Benson, E.; Nyström, A. M.; Högberg, B. DNA Origami Delivery System for Cancer Therapy with Tunable Release Properties. *ACS Nano* **2012**, 8684–8691.
6. Perrault, S. D.; Shih, W. M. Virus-Inspired Membrane Encapsulation of DNA Nanostructures To Achieve *in Vivo* Stability. *ACS Nano* **2014**, 5132–5140.
7. Kuzyk, A.; Schreiber, R.; Fan, Z.; Pardatscher, G.; Roller, E.-M.; Högele, A.; Simmel, F. C.; Govorov, A. O.; Liedl, T. DNA-Based Self-Assembly of Chiral Plasmonic Nanostructures with Tailored Optical Response. *Nature* **2012**, *483*, 311–314.
8. Klein, W. P.; Schmidt, C. N.; Rapp, B.; Takabayashi, S.; Knowlton, W. B.; Lee, J.; Yurke, B.; Hughes, W. L.; Graugnard, E.; Kuang, W. Multiscaffold DNA Origami Nanoparticle Waveguides. *ACS Nano* **2013**, *47*, 1778–1788.
9. Bellot, G.; McClintock, M. A.; Chou, J. J.; Shih, W. M. DNA Nanotubes for NMR Structure Determination of Membrane Proteins. *Nat. Protoc.* **2013**, *8*, 755–770.
10. Derr, N. D.; Goodman, B. S.; Jungmann, R.; Leschziner, A. E.; Shih, W. M.; Reck-Peterson, S. L. Tug-of-War in Motor Protein Ensembles Revealed with a Programmable DNA Origami Scaffold. *Science* **2012**, *338*, 662–665.
11. Langecker, M.; Arnaut, V.; Martin, T. G.; List, J.; Renner, S.; Mayer, M.; Dietz, H.; Simmel, F. C. Synthetic Lipid Membrane Channels Formed by Designed DNA Nanostructures. *Science* **2012**, *338*, 932–936.
12. Tørring, T.; Helmig, S.; Ogilby, P. R.; Gothelf, K. V. Singlet Oxygen in DNA Nanotechnology. *Acc. Chem. Res.* **2014**, *47*, 1799–1806.
13. Voigt, N. V.; Tørring, T.; Rotaru, A.; Jacobsen, M. F.; Ravnsbaek, J. B.; Subramani, R.; Mamdouh, W.; Kjems, J.; Mokhir, A.; Besenbacher, F.; *et al*. Single-Molecule Chemical Reactions on DNA Origami. *Nat. Nanotechnol.* **2010**, *5*, 200–203.
14. Shaw, A.; Lundin, V.; Petrova, E.; Fördos, F.; Benson, E.; Al-Amin, A.; Herland, A.; Blokzijl, A.; Högberg, B.; Teixeira, A. I. Spatial Control of Membrane Receptor Function Using Ligand Nanocalipers. *Nat. Methods* **2014**, *11*, 841–846.
15. Douglas, S. M.; Bachelet, I.; Church, G. M. A Logic-Gated Nanorobot for Targeted Transport of Molecular Payloads. *Science* **2012**, *335*, 831–834.
16. Schüller, V. J.; Heidegger, S.; Sandholzer, N.; Nickels, P. C.; Suhartha, N. A.; Endres, S.; Bourquin, C.; Liedl, T. Cellular Immunostimulation by CpG-Sequence-Coated DNA Origami Structures. *ACS Nano* **2011**, *5*, 9696–9702.
17. Lin, C.; Perrault, S. D.; Kwak, M.; Graf, F.; Shih, W. M. Purification of DNA-Origami Nanostructures by Rate-Zonal Centrifugation. *Nucleic Acids Res.* **2013**, *41*, e40.
18. Jeyachandran, Y. L.; Mielczarski, J. A.; Mielczarski, E.; Rai, B. Efficiency of Blocking of Non-Specific Interaction of Different Proteins by BSA Adsorbed on Hydrophobic and Hydrophilic Surfaces. *J. Colloid Interface Sci.* **2010**, *341*, 136–142.
19. Steinhauer, C.; Jungmann, R.; Sobey, T. L.; Simmel, F. C.; Tinnefeld, P. DNA Origami as a Nanoscopic Ruler for Super-Resolution Microscopy. *Angew. Chem., Int. Ed.* **2009**, *48*, 8870–8873.
20. Woller, J. G.; Hannestad, J. K.; Albinsson, B. Self-Assembled Nanoscale DNA–Porphyrin Complex for Arti Fi Cial Light Harvesting. *J. Am. Chem. Soc.* **2013**, 2759–2768.
21. Lin, C.; Jungmann, R.; Leifer, A. M.; Li, C.; Levner, D.; Church, G. M.; Shih, W. M.; Yin, P. Submicrometre Geometrically Encoded Fluorescent Barcodes Self-Assembled from DNA. *Nat. Chem.* **2012**, *4*, 832–839.
22. Schmied, J. J.; Raab, M.; Forthmann, C.; Pibiri, E.; Wünsch, B.; Dammeyer, T.; Tinnefeld, P. DNA Origami-Based Standards for Quantitative Fluorescence Microscopy. *Nat. Protoc.* **2014**, *9*, 1367–1391.
23. Bennett, K. M.; Shapiro, E. M.; Sotak, C. H.; Koretsky, A. P. Controlled Aggregation of Ferritin to Modulate MRI Relaxivity. *Biophys. J.* **2008**, *95*, 342–351.
24. Tan, S. C.; Yiap, B. C. DNA, RNA, and Protein Extraction: The Past and the Present. *J. Biomed. Biotechnol.* **2009**, *2009*, 574398.
25. Douglas, S. M.; Chou, J. J.; Shih, W. M. DNA-Nanotube-Induced Alignment of Membrane Proteins for NMR Structure Determination. *Proc. Natl. Acad. Sci. U.S.A.* **2007**, *104*, 6644–6648.
26. Stahl, E.; Martin, T. G.; Praetorius, F.; Dietz, H. Facile and Scalable Preparation of Pure and Dense DNA Origami Solutions. *Angew. Chem., Int. Ed.* **2014**, 1–7.
27. Bellot, G.; McClintock, M. A.; Lin, C.; Shih, W. M. Recovery of Intact DNA Nanostructures after Agarose Gel-Based Separation. *Nat. Methods* **2011**, *8*, 192–194.
28. Wickham, S. F. J.; Endo, M.; Katsuda, Y.; Hidaka, K.; Bath, J.; Sugiyama, H.; Turberfield, A. J. Direct Observation of Stepwise Movement of a Synthetic Molecular Transporter. *Nat. Nanotechnol.* **2011**, *6*, 166–169.
29. Yurke, B.; Turberfield, A. J.; Mills, A. P., Jr.; Simmel, F. C.; Neumann, J. L. A DNA-Fuelled Molecular Machine Made of DNA. *Nature* **2000**, *406*, 605–608.
30. Tharmalingam, T.; Ghebeh, H.; Wuerz, T.; Butler, M. Pluronic Enhances the Robustness and Reduces the Cell Attachment of Mammalian Cells. *Mol. Biotechnol.* **2008**, *39*, 167–177.
31. Ducani, C.; Kaul, C.; Moche, M.; Shih, W. M.; Högberg, B. Enzymatic Production of "Monoclonal Stoichiometric" Single-Stranded DNA Oligonucleotides. *Nat. Methods* **2013**, *10*, 647–652.